RSC Advances

ROYAL SOCIETY OF CHEMISTRY

www.rsc.org/advances

Highly selective zirconia-based propene sensor attached with sol-gel derived NiO nanospheres

Kamaraj Mahendraprabhu and Perumal Elumalai*

Electrochemical Energy and Sensors Lab
Department of Green Energy Technology
Madanjeet School of Green Energy Technologies
Pondicherry University, Puducherry-605014, India.

Abstract

Nanospheres of nickel oxide (NiO) were synthesized by a simple modified sol-gel route using nickel nitrate as precursor and citric acid as gelling agent. Yttria-stabilized zirconia (YSZ)-based sensor was fabricated using the sol-gel derived NiO nanospheres as sensing electrode (SE) and Pt as reference electrode (RE), and its sensing characteristics were examined in the temperature range of 650-800°C under various O_2 concentrations (5, 10, 15 and 21 vol %). The fabricated NiO-SE was characterized by X-ray diffraction (XRD) and scanning electron microscope (SEM). It turned out that the sensor attached with the sol-gel derived NiO-SE exhibited selective and sensitive response to propene (C_3H_6) at 700°C in all measured O_2 concentrations. The sensor showed the highest sensitivity and selectivity to propene in 21 vol % O_2. In addition, the sensor exhibited stable response to C_3H_6 for about two months. The sensing mechanism was confirmed to be mixed-potential-type. It is believed that the nanofeatures associated with the sol-gel derived NiO seemed to be responsible for high sensitivity and selectivity to C_3H_6.

Keywords: Sol-gel; NiO; YSZ; Mixed potential; Propene sensor

*Corresponding author. Tel.: +91-413-2654867; Fax: +91-413-2656758
E-mail: drperumalelumalai@gmail.com; elumalai.get@pondiuni.edu.in (P. Elumalai)

1. Introduction

In the recent decades, human have gained a notable rise in their living standards due to increased and modernized industrialization including automobile industries. Although the industrialization and modernization led to a lot of positive impacts, they have also lead to severe environmental issues, especially air pollution, caused by the expanding usage of automobiles. Among the various types of pollutions, air pollution poses a challenging factor in the living environment. In fact, various toxic pollutants such as, NO_x ($NO + NO_2$), CO, SO_x and unburnt hydrocarbons (HCs) including propane, propene etc., are released from the industries and the automobiles, leading to adverse effects such as acid rain, ozone depletion, green-house effect, photochemical smog, etc[1-3]. Among the various sources, combustion of fossil fuels in the industries and in the automobiles is the major source for the air pollution. The one way to control the toxic emissions from the automobiles is to make sure the presence of required air to fuel ratio (A/F) for efficient fuel combustion with the help of feedback control unit equipped with emission monitoring systems. The other way to reduce the toxic emissions is to use post cylinder de-emission technologies. Currently, stringent emission legislations such as Euro VI (Europe), Tier-3 (USA) and BS-IV (India) should be enforced in the automobiles to monitor the toxic emissions. For example, the Euro VI and BS-IV set the NO_x, CO and HCs emission limits to be 0.06, 0.5, 0.1 g/km, respectively[4-6]. Thus, the automobile manufacturers are forced to adopt de-emission technology equipped with feedback control unit having emission monitoring system. To meet such stringent norms, it is important to develop high performance NO_x, CO and HCs sensors which would work well at elevated temperatures of above 500^oC under harsh conditions such as varying O_2, CO_2 and H_2O concentrations [6-7].

Recently, electrochemical sensors using high temperature solid electrolyte, namely yttria-stabilized zirconia (YSZ) have received great attention for detecting various analytes as they can work well even in the aforesaid harsh environments. Currently, several reports on YSZ-based sensors operating at different modes such as mixed potential, impedancemetric and

amperometric are reported [6-8]. Among them, mixed-potential-type sensor is preferred due to its attractive features such as high sensitivity, portability and low cost [9-10].

As sensing electrode (SE) materials, metals, metal oxides and composites have been utilized and their sensing performances were reported[11-14]. For example, Dutta *et al.,* reported the use of WO_3 to detect NO_2 and CO gases[15]. Diao *et al.,* utilized $MnCr_2O_4$ as NO_2 sensing material. Sintering temperature of $MnCr_2O_4$ was modulated and it was reported that $MnCr_2O_4$ sample sintered at 1000°C exhibited higher response to NO_2 gas[16]. Quite recently, Zhou *et al.,* optimized the sintering temperature of $(La_{0.8}Sr_{0.2})_2FeMnO_{6-\delta}$ and the sensor sintered at 1200°C showed the high sensitivity to NO_2 at 550°C[17]. Park *et al.,* used each of NiO, CuO and NiO (+YSZ) as sensing electrodes for sensing total NO_x concentration[18]. Liang *et al*., utilized NiO as sensing material and reported the improvement in the NO_2 sensitivity by tuning triple-phase boundary using hydrofluoric acid (HF), and the sensor showed higher sensitivity to NO_2 using YSZ treated with 40% HF[19]. The use of metal/metal oxide composite as SEs showed higher sensitivity than individual metals and metal oxides. For example, Westphal *et al*., utilized composite consisting of Ga_2O_3 and Au for sensing of hydrocarbons[20]. Wang *et al*., used composite consisting of NiO and Rh for sensing of NO_x gas. The NiO added with 3 wt % Rh showed higher response to NO_2 compared with pure NiO[21]. The NiO-Au composite was found to exhibit selective response to propene, while the pure NiO and Au are not so selective[22].. In most of above cases, commercial oxide was utilized. To the best of our knowledge, the influence of synthetic process on the sensing performance was not explored for NiO. Thus, in the present work, NiO nanospheres were synthesized by using a simple modified sol-gel route and characterized by powder X-ray diffraction (XRD) and scanning electron microscope (SEM). The obtained NiO was used for fabrication of YSZ-based mixed-potential-type sensor and its gas sensing properties are reported here.

2. Experimental

2.1 Sol-gel synthesis of NiO

Nickel oxide nanospheres were synthesized by a simple citrate-based sol-gel method by using nickel nitrate as precursor and citric acid as a gelling agent. The detailed synthesis and influence of citric acid concentration on the formation of sol-gel end products have been reported by us recently elsewhere[23]. However, brief sol-gel process for synthesis of NiO nanospheres is described here. Nickel nitrate and citric acid in 1:8 mole ratio was used for synthesis of NiO. Required quantity of nickel nitrate was dissolved in distilled water and kept at 80°C on a magnetic stirrer. The required amount of citric acid was also dissolved in distilled water separately. To the warm nickel nitrate solution, citric acid solution was added in dropwise. After the complete addition of all citric acid, the content was heated to 130°C to form sol and continued heating to get gel. The formed gel was allowed to dry at 130°C for overnight. The calcination of the gel at 500°C for 2 h in air was done to get the final product.

2.2 Fabrication of sensor device

The YSZ-based sensor was made up of a one-end-opened commercially available YSZ tube (8 mol.% Y_2O_3-doped zirconia) as solid electrolyte (oxide-ion conductor), the above synthesised NiO as sensing electrode (SE) and Pt as reference electrode (RE). The YSZ tube had 300 mm length and inner diameter of 9 mm. For fabrication of NiO-SE and Pt-RE, each of NiO and Pt powders (Ants Ceramics, India) were mixed with α-terpineol solvent in an agate mortar to make uniform paste. The obtained pastes were applied on the outer surface of the YSZ tube and dried at 110°C for 6 h in air and subsequently sintered at 1300°C for 2 h in air. After the sintering, 0.4 mm thickness Pt wire was wound on each of the NiO and Pt layers for the purpose of current collectors. Then, the sensor was housed in a quartz tube. Fig. 1 shows the photograph of exteria of the fabricated YSZ-based sensor device. The crystal structure of sintered NiO layer formed on the YSZ was determined by means of X-ray diffraction analysis (XRD Diffractometer, Bruker D8

Advanced) using CuK_α source (λ=1.5418 Å). The surface morphology of the NiO layer was observed by means of scanning electron microscope (SEM/EDX - Hitachi S3400N).

2.3 Evaluation of gas sensing properties

The evaluation of gas sensing characteristics of the fabricated sensor was carried out in a homemade gas-flow apparatus equipped with digital mass-flow controllers and a furnace operating in the temperature range of 650-800°C. The required concentration of propene sample gas was prepared by diluting a commercially-available propene (1000 *ppm* propene gas + N_2 balance) with nitrogen and was allowed to flow over the sensor surface at a constant flow rate of 100 cm^3 min^{-1}. The *ppm* refers to the volume concentration of the gaseous mixture. The potential difference (*emf*) between NiO-SE and Pt-RE of the sensor was measured with a digital electrometer (GWINSTEK, GDM-8261). Cross sensitivities to each of 400 ppm NO_2, NO, CO, C_3H_8 and C_3H_6 were measured at 700°C. All the measurements were performed under dry condition. Base gas refers to the mixture of O_2 and N_2 gas in a desired proportion (5, 10, 15 and 21 vol % O_2 + N_2 balance). Sample gas refers to the mixture of target gas (in desired concentration) and the base gas.

The current-voltage (polarization) curves of the sensor were measured by using source meter (Agilent technologies, model: B2900A) based on a potential-sweep method at a scan rate of 2 mVs^{-1} in the base gas (5 or 21 vol % O_2 + N_2 balance) and in the sample gas (400 *ppm* C_3H_6 + base gas). The current of the cathodic polarization curve (measured in base gas) was subtracted from that of the anodic polarization curve (measured in sample gas) at each potential, so as to obtain the modified-anodic polarization curve in which the current axis is expressed in an absolute scale.

3. Results and Discussion

3.1 Crystal structure and morphology of SE layer

Figure 2 shows the XRD pattern of NiO layer on YSZ substrate sintered at 1300°C. For comparison, the XRD pattern obtained on pure YSZ substrate is also given. The set of Bragg peaks obtained for YSZ substrate could be conveniently indexed to cubic phase of YSZ as per the JCPDS # 772112. In the case of oxide on YSZ, the set of Bragg peaks appeared at 30.09,

34.94, 50.19, 59.59, 62.39, 73.57, 81.71, and 84.25° correspond to the XRD pattern of cubic YSZ, while the set of Bragg peaks appeared at 37.04, 43.04, 75.28 and 79.29° could be indexed to the face centered cubic NiO as per the JCPDS # 731519. No other impurity peaks were observed. Thus, the XRD results confirmed that even after sintering at 1300°C, nickel oxide is stable and could exist on YSZ substrate. It is known that the melting point of NiO is above 1900°C which is away from the sintering temperature used in the present fabrication process. The crystallite size of NiO estimated from the Bragg peak (43.04°) was about 142 nm using Scherer formula given below.

$$L_{hkl} = 0.9 \lambda / \beta \cos \theta$$

Where, L_{hkl} denotes crystallite size, λ is X-ray wavelength (1.5418 Å), β is the full width at half maximum (FWHM) of the Bragg peak (in radians), and θ is the Bragg angle. Figure 3 shows the surface morphology of 1300°C-sintered NiO layer. The surface consists of uniform and spherical shape of NiO grains with interconnections throughout the matrix (Fig. 3(b)). The surface also consists of uniform pores with the pore size varying from 80 to 350 nm. The NiO grain size is about 180 nm. It is expected that these nano-grains and pores would influence on the sensing performance of the sensor.

3.2 Sensing performances of the sensor

To examine the sensing performances of the sensor attached with 1300°C-sintered NiO-SE, cross sensitivities to various gases such as NO_2, NO, CO, C_3H_8 (propane) and C_3H_6 (propene) were measured in each of 5, 10, 15 and 21 vol. % base gas (O_2 + N_2 balance) at 700°C. Figure 4 shows the comparison of the obtained cross sensitivities of the sensor. The cross sensitivity (Δemf) is defined as the difference between the emf value in the sample gas and that in the base gas, as shown below,

$$\Delta emf = emf_{sample} - emf_{base\ gas}$$

It is seen that the sensor showed high sensitivity and selectivity to propene in each of the examined oxygen concentration. It is noted that the cross sensitivities to all other gases are much

less than that of the propene, irrespective of oxygen concentration. As the oxygen concentration is increased the sensitivity to propene also increased, and the highest sensitivity and selectivity was observed in 21 vol % O_2. Thus, among the various oxygen concentrations examined, 21 vol. % O_2 is optimum to obtain high sensitivity and selectivity. It is noteworthy that the oxygen concentration in the air is 21 vol. % and that in the automobile exhaust is almost 5 vol. %. Thus, the present sensor can be used in practical exhaust with control unit for oxygen concentration. Even under 5 vol. % base gas, the sensitivity and selectivity are quite good.

Since the sensor attached with the sol-gel derived NiO-SE exhibited selective response to C_3H_6, further C_3H_6 sensing characteristics were examined in detail. Fig. 5 shows response transients to C_3H_6 in the concentration range of 10-400 ppm at 700°C for the sensor attached with the sol-gel derived NiO-SE. The emf of the sensor in the base gas was almost constant and changed quickly from the base value, and then reached almost steady-state value in due course of time. The sensor returned to the original base value upon changing the base gas to the sample gas at each concentration. It can be seen that the steady-state emf of the sensor increased with increase of C_3H_6 concentration, showing excellent sensing ability of the sensor to varying concentrations. It is worthy to note that sensor showed good response to even very low concentration of C_3H_6 (10 ppm). Response time is the time taken to reach the saturation emf while changing from base gas to sample gas, where as recovery time refers the time taken for returning to the original base value while changing from the sample gas to the base gas. For a practical sensor, response/recovery rates are important key factors. Thus, the estimated 80% response/recovery times of the sensor were about 60s/120s. It was observed that the response and recovery times were same for all the propene concentrations except for 10 ppm, it was quicker. It can be seen that the sensor would have taken few more seconds to reach saturation emf. However, the constant duration was kept for registering sensing signals in each of propene concentration.

It is noted that the flow rate in our experiments was only 100 cm^3 min^{-1}. But, in the actual exhaust, the flow rate is much higher. Thus, the present sensor is expected to show much faster response/recovery rates in actual exhaust.

The temperature of the automobile exhaust is dynamic, it goes even upto 800°C and will play a significant role in deciding the sensitivity of the sensor. Thus, it is important to examine the sensitivity of the sensor at various operating temperatures. To examine the influence of operating temperature on the C_3H_6 sensitivity, the response transients to various concentrations of C_3H_6 was recorded at each of 650°C, 700°C, 750°C and 800°C. From the obtained response transients, the sensitivity to each C_3H_6 concentration was calculated by using following equation.

$$\Delta emf = emf_{propene} - emf_{base\ gas}$$

Figure 6 shows the dependence of Δemf on the concentration of C_3H_6 at each of 650°C, 700°C, 750°C and 800°C. It can be seen that the Δemf varies linearly with C_3H_6 concentrations on the logarithmic scale at each temperature although with slight change in the slope. Such a linear dependence of Δemf on the logarithmic scale is characteristics for mixed-potential-type sensor, as has been reported elsewhere[6-10]. It is noteworthy that, as the operating temperature is increased, the sensitivity to C_3H_6 decreases significantly (Note: sign of Δemf). The more negative Δemf could be due to increased rate of C_3H_6 anodic reaction at elevated temperature. It is noted that even at 800°C, the sensitivity to 400 ppm C_3H_6 is about -98 mV which is highly desirable.

The long-term stability of the sensor is one of the vital parameters for a practical sensor. Thus, to examine the stability, sensitivity to 400 ppm C_3H_6 for the sensor attached with the sol-gel derived NiO-SE was monitored for about two months and the obtained data are given in Figure 7. On the first day of sensor operation, the sensor was exhibited the sensitivity of about -98 mV and at the end of two months, the sensor retained as high as 90 % (-88 mV) of its original (-98 mV) sensitivity. The response/recovery rates were also almost invariant as depicted in inset of Fig. 7. Thus, the present sensor using the sol-gel derived NiO-SE exhibits excellent stability

even for about two months and could be a potential candidate for practical application in automobile exhausts.

3.3 Sensing mechanism and estimation of mixed potential

Though the YSZ tube was used, the sensor configuration of the present work can be best described as planar sensor and its electrochemical cell configuration is shown below:

$$21\ \text{vol \%}\ O_2, NiO\ |YSZ|\ Pt, 21\ \text{vol \%}\ O_2 \qquad \text{(in base gas)}$$

$$C_3H_6 + 21\ \text{vol \%}\ O_2, NiO\ |YSZ|\ Pt, 21\ \text{vol \%}\ O_2 + C_3H_6 \qquad \text{(in sample gas)}$$

Based on the aforementioned results and the available literature reports, the sensing mechanism operating in the present sensor is seemed to be mixed potential mechanism. In the base gas, the following electrochemical reaction will be equilibrating at both the electrodes.

$$O^{2-} = \tfrac{1}{2}O_2 + 2e^- \qquad (1)$$

On the other hand, in the sample gas, the following two competitive electrochemical reactions would be occurring simultaneously at the interface of NiO/YSZ.

$$\tfrac{1}{2}O_2 + 2e^- \rightarrow O^{2-} \quad \text{(Cathodic)} \qquad (2)$$

$$C_3H_6 + 9O^{2-} \rightarrow 3CO_2 + 3H_2O + 18e^- \quad \text{(Anodic)} \qquad (3)$$

As the rate of these two electrochemical reactions are different at dissimilar electrodes (NiO-SE and Pt-RE), mixed potential appears when the rate of anodic reaction is equal to that of cathodic reaction which is recorded in the response transients. The appearance of the mixed potential can be estimated from the polarization curves. In fact, the mixed potential can be defined as the potential where the cathodic and anodic polarization-curves intersect in an absolute current scale. Thus, the polarization (current-voltage, I-V) curves for the sensor attached with the sol-gel derived NiO-SE were measured in the base gas (5 vol.% O_2 + N_2 balance or 21

vol.% O_2 + N_2 balance) and in the sample gas (400 ppm C_3H_6 + base gas) at 700°C. Fig. 8 shows the obtained I-V curves. It can be seen that in the 5 vol.% O_2 base gas, the estimated mixed potential (-43 mV) is in close coincidence with that of the observed emf (-40 mV). Similarly, in the 21 vol.% O_2 base gas, the estimated mixed potential is -94 mV which is close to the observed emf (-98 mV). Such close coincidence of the observed and the estimated emf values confirms that the mechanism of the present sensor is based on mixed potential.

The change in sensitivity of the sensor with varying base gas was examined with the help of I-V curves. In fact, from the I-V curves, it can be inferred that higher the polarization current, higher the reaction rate and vice versa. Thus, as is evident, the polarization current of 400 ppm C_3H_6 obtained in 21 vol. % O_2 is higher than that obtained in 5 vol. % O_2. It means that the rate of anodic reaction of C_3H_6 is higher in 21 vol. % O_2 than that in 5 vol. % O_2. Thus, accordingly anodic polarization curve of C_3H_6 shifts upward when the base gas is changed from 5 vol. % O_2 to 21 vol. % O_2, leading to drastic shift in the mixed potential. The high C_3H_6 sensitivity and selectivity of the sensor using the sol-gel derived NiO-SE is believed to be due to the improved kinetics of C_3H_6 anodic reaction because of nanofeature associated with the sol-gel derived NiO-SE. It is assumed that on the NiO layer, the other gases NO, CO, C_3H_8 and NO_2 are decomposed to maximum extent before reaching the NiO/YSZ interface, leading to high C_3H_6 selectivity. "The commercial NiO (morphology: size, shape and size distribution are different and hence is sensing properties) is not selective to propene[24-25]. Interestingly, the present sensor attached with sol-gel derived NiO nanospheres exhibited excellent selectivity, sensitivity and stability to propene. There are other materials showing response to propene, but it is not a single material, a composite, consisting of oxide and expensive gold[22], besides NiO being thermally stable material and non-toxic with high electrocatalytic activity to propene. In these views, the present sensor has high significance."

4. Conclusions

YSZ-based sensor was fabricated using the sol-gel derived NiO nanospheres. The sensor attached with the sol-gel derived NiO-SE showed high sensitivity and selectivity to C_3H_6 at 700°C in 21 vol % O_2. The Δemf of the sensor varied linearly with C_3H_6 concentrations on the logarithmic scale. The sensor exhibited excellent response to even very low concentration of C_3H_6 (10 ppm). The sensor retained good stability even for about two months. Thus, the sensor attached with the sol-gel derived NiO-SE can be a reliable propene sensor although sensing characteristics under wet condition and varying flow rates are to be examined.

Acknowledgements

Authors thank Department of Science and Technology (DST), Govt. of India, New Delhi for financial support under Fast-Track Scheme (DST/FT/CS-64/2010). CSIR-CECRI (Karaikudi and Chennai) and the Central Instrumentation Facility - Pondicherry University also acknowledged for characterization studies.

References

1. T. Watson, Nature, 2014, **513**, S14-15.
2. M. Kampa, E. Castanas, Environ Pollut., 2008, **15**, 362-367.
3. B. M. Graver, H.C. Frey, H. W Choi, Environ Sci Technol., 2011, **45**, 9044-9051.
4. S. Zhuiykov, N. Miura, Sens. Actuators. B: Chem., 2007, **121**, 639-651.
5. P. K. Sekhar, E.L. Brosha, R. Mukundan, W. Li, M.A. Nelson, P. Palanisamy, F.H. Garzon, Sens. Actuators. B: Chem., 2010, **144**, 112-119.
6. N. Miura, T. Sato, S.A. Anggraini, H. Ikeda, S. Zhuiykov, Ionics, 2014, **20**, 901-925.
7. Y. Liu, J. Parisi, X. Sun, Y. Lei, J. Mater. Chem. A, 2014, **2**, 9919- 9943.
8. J.W. Fergus, Sens. Actuators. B: Chem., 2007, **122**, 683-693.
9. G. Lu, Q. Diao, C. Yin, S. Yang, Y. Guan, X. Cheng, X. Liang, Solid State Ionics 2014, **262**, 292-297.
10. X. Xu, X. Li, W. Wang, B. Wang, P. Sun, Y. Sun, G. Lu, RSC Adv.**,** 2014, **4**, 4831-4835.
11. J.S. Narayanan, M. Bhuvana, V. Dharuman**,** Biosens. Bioelectron., 2014, **58**, 326-332.
12. Y. Fujio, T. Sato, N. Miura, Solid State Ionics, 2014, **262**, 266-269.
13. J.W. Fergus, Sens. Actuators. B: Chem., 2007, **121**, 652-663.
14. K. Mahendraprabhu, N. Miura, P. Elumalai, Ionics, 2013, **19**, 1681-1686.
15. A. Dutta, N. Kaabbuathong, M.L. Grilli, E.D. Bartolomeo, E. Traversa, J. Elecrochem. Soc., 2003, **150**, H33-H37.
16. Q. Diao, C. Yin, Y. Guan, X. Liang, S. Wang, Y. Liu, Y. Hu, H. Chen, G. Lu, Sens. Actuators. B: Chem., 2013, **177**, 397-403.
17. L. Zhou, Quan Yuan, Xiangdong Li, Juanjuan Xu, Feng Xia, Jianzhong Xiao, Sens. Actuators. B: Chem., 2015, **206,** 311-318.
18. J. Park, B.Y. Yoon, C.O. Park, W.J. Lee, C.B. Lee, Sens. Actuators. B: Chem., 2009, **135**, 516-523.

19. X. Liang, S. Yang, J. Li, H. Zhang, Q. Diao, W. Zhao, G. Lu, Sens. Actuators. B: Chem., 2011, **158**, 1-8.

20. D. Westphal, S. Jakobs, U. Guth, Ionics, 2001, **7**, 182-186.

21. J. Wang, P. Elumalai, D. Terada, M. Hasei, N. Miura, Solid State Ionics, 2006, **177**, 2305-2311.

22. P. Elumalai, V.V. Plashnitsa, Y. Fujio, N Miura, Sens. Actuators. B: Chem., 2010, **144**, 215-219.

23. K. Mahendraprabhu, P. Elumalai, J. Sol-Gel Sci. Technol., 2015, **73,** 428-433.

24. P. Elumalai, J. Wang, S. Zhuiykov, D. Terada, M. Hasei, N. Miura, J. Electrochem Soc., 2005, **152**, H95-H101.

25. P. Elumalai, N. Miura, Solid State Ionics, 2005, **176**, 2517-2522.

Figure Captions

Fig. 1. Photograph of the exteria of the assembled YSZ-based sensor attached with the sol-gel derived NiO-SE and Pt-RE.

Fig. 2. XRD patterns of (a) YSZ substrate and (b) the sol-gel derived 1300°C-sintered NiO-SE layer on YSZ substrate.

Fig. 3. SEM images at (a) low magnification and (b) high magnification on surface of 1300°C-sintered NiO-SE layer.

Fig. 4. Cross sensitivities to various gases for the YSZ-based sensor attached with the sol-gel derived NiO-SE at 700°C under dry condition.

Fig. 5. Response transients to various concentration of C_3H_6 for the YSZ-based sensor attached with the sol-gel derived NiO-SE at 700°C.

Fig. 6. Dependence of Δemf on the concentration of C_3H_6 at various operating temperatures for the YSZ-based sensor attached with the sol-gel derived NiO-SE.

Fig. 7. Time course of Δemf to 400 ppm C_3H_6 at 700°C for the YSZ-based sensor attached with the sol-gel derived NiO-SE (Inset: Response transients of the sensor on first and sixtieth day of operation).

Fig. 8. Anodic polarization curves of C_3H_6 and modified cathodic polarization-curves of 5 and 21 vol.% O_2 at 700°C for the sensor attached with the 1300°C-sintered NiO-SE.

Mahendraprabhu and Elumalai

Figure 1

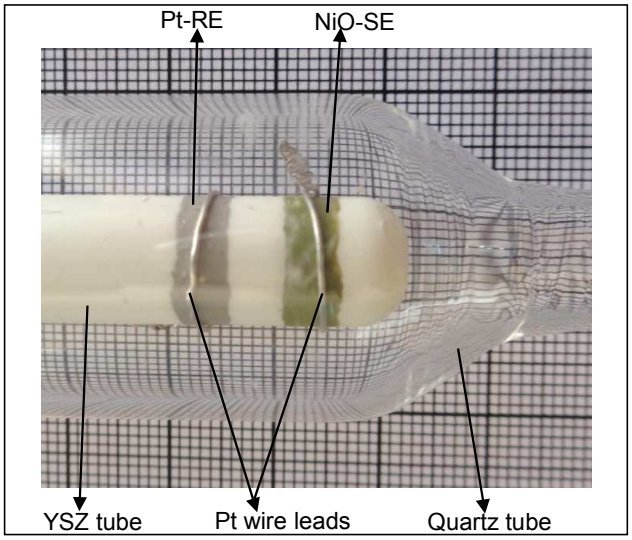

Mahendraprabhu and Elumalai

Figure 2

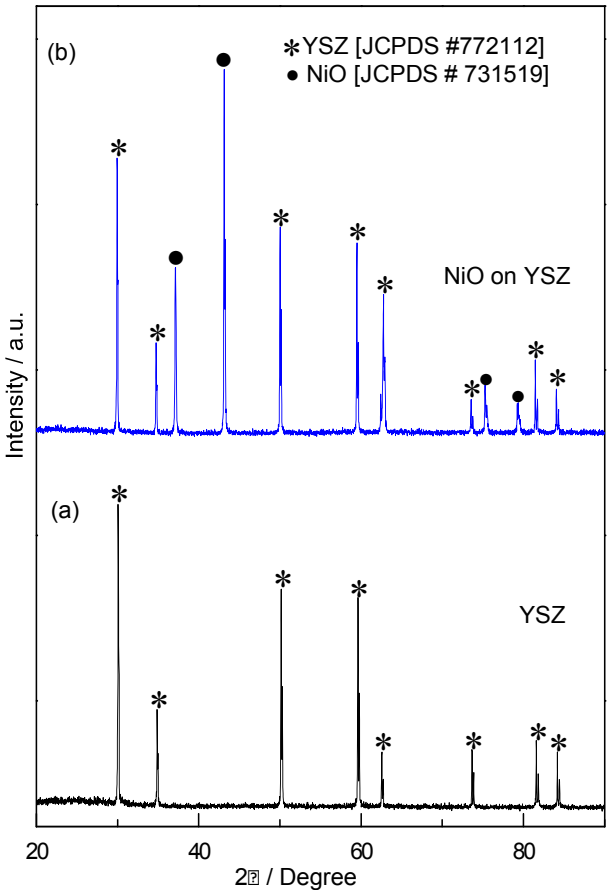

Figure 3

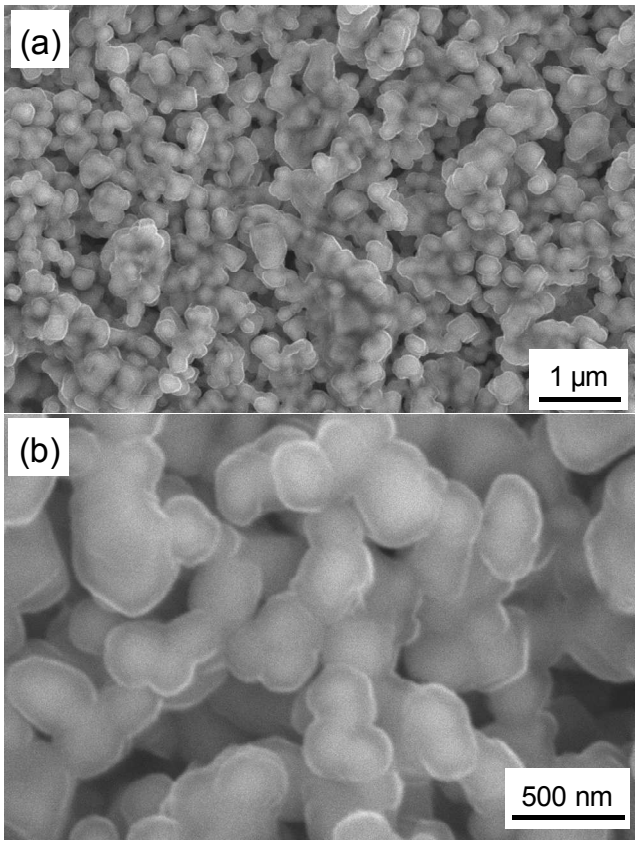

Figure 4

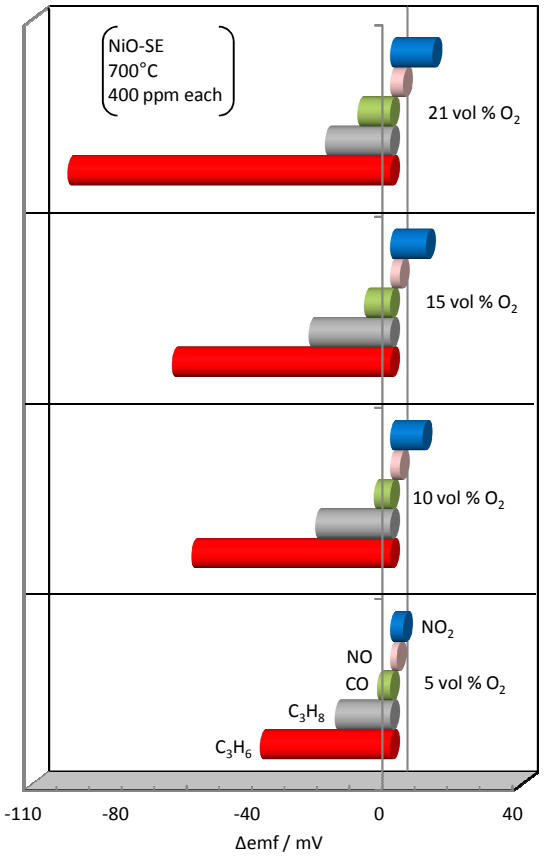

Mahendraprabhu and Elumalai

Figure 5

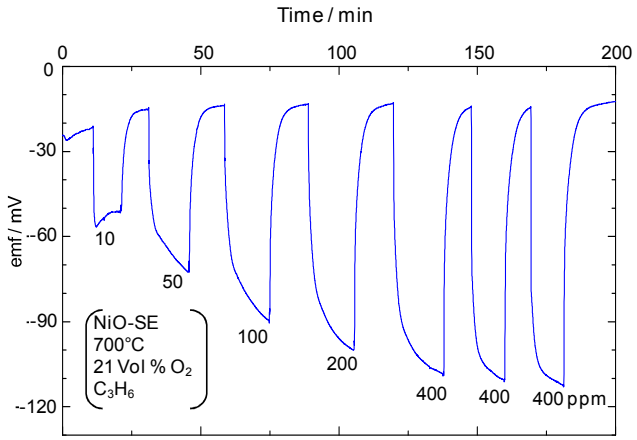

Figure 6

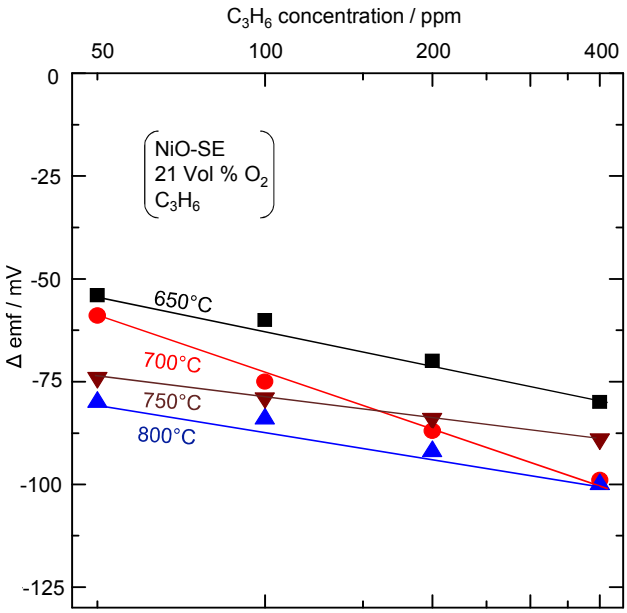

Figure 7

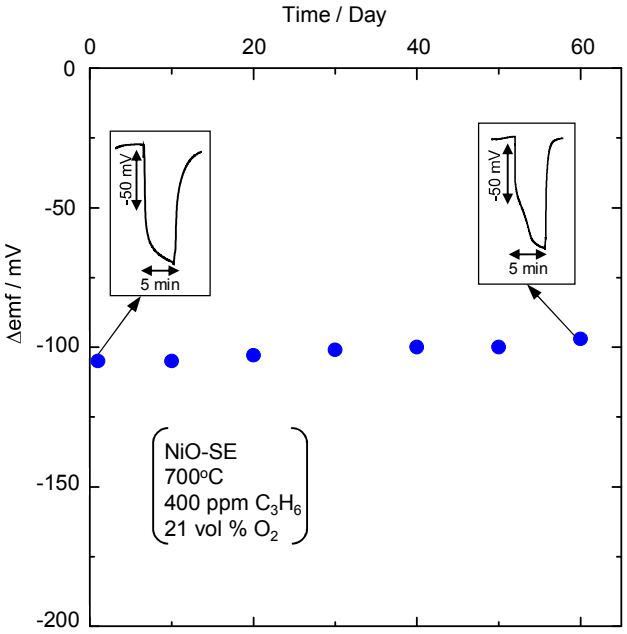

Mahendraprabhu and Elumalai

Figure 8

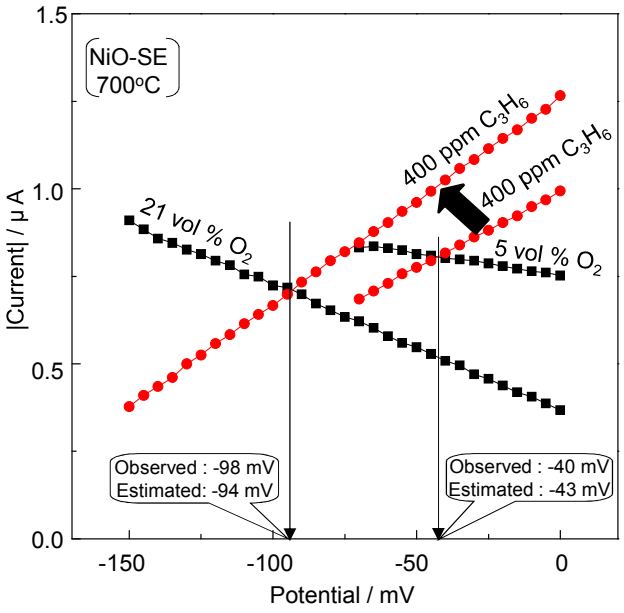

Justification

High-performance yttria-stabilized zirconia (YSZ)-based electrochemical gas sensors are highly demanding for detection of automobile exhaust gases such as NO, CO, C_3H_6, C_3H_8 and NO_2 at high temperature. In the present work, YSZ-based sensor was fabricated using sol-gel derived NiO nanospheres. It turned out that the present sensor exhibited high sensitivity and selectivity to C_3H_6 (propene) with good long term stability. Based on the type of materials used and the topic of the work, this manuscript is highly suitable for publication in *RSC Advances* under "Environmental" subject.

Highlights:

- YSZ-based electrochemical sensor was fabricated using sol-gel derived NiO nanospheres.
- The sensor exhibited high sensitivity and selectivity to C_3H_6.
- The sensor showed good response to even very low concentration of C_3H_6 (10 ppm).
- The sensor attached with sol-gel derived NiO sensing-electrode exhibited good long-term stability.

Graphical Abstract
Mahendraprabhu and Elumalai

Highly selective zirconia-based propene sensor attached with sol-gel derived NiO nanospheres

K. Mahendraprabhu and P. Elumalai

YSZ-based electrochemical sensor was fabricated using sol-gel derived NiO nanospheres. The sensor exhibited high sensitivity and selectivity to C_3H_6 (propene) with excellent long-term stability.